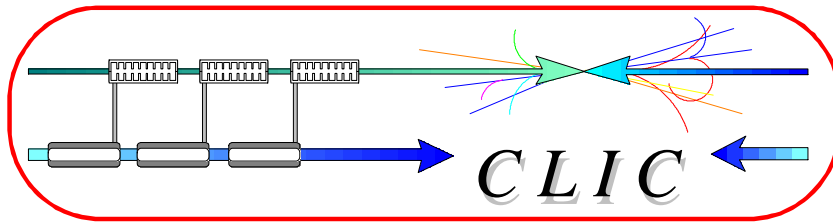


# CERN - European Laboratory for Particle Physics



**CLIC Note 298**  
**08. 03. 1996**

**NLC-Note 20**  
**Distribution:**  
**Sources/Injectors**  
**SLAC, 8 March 1996**

## RF Guns and the Production of Polarized Electrons

K. Aulenbacher<sup>†</sup>, R. Bossart<sup>†</sup>, H. Braun<sup>†</sup>, J. Clendenin<sup>†#</sup>, J.P. Delahaye<sup>†</sup>, J. Madsen<sup>†</sup>, G. Mulhollan<sup>‡</sup>,  
J. Sheppard<sup>‡</sup>, G. Suberlucq<sup>†</sup>, and H. Tang<sup>‡</sup>

<sup>†</sup>CERN  
1211 Geneva 23

<sup>‡</sup>Stanford Linear Accelerator Center  
Stanford, CA 94025

### 1. Motivation

Future electron colliders will presumably require polarized electrons and possibly even polarized positrons. Linear colliders in particular must rely on external sources to produce polarized electrons (although there are proposals for producing polarized electrons using helical undulators or polarized Compton backscattering--both requiring incident electrons with energy  $>150$  GeV). In recent years there has been rapid progress in solid-state polarized electron sources as exemplified by the source at SLAC[1]. The value of a load-lock system is now obvious. In addition, much of the SLAC experience is applicable to a polarized rf gun. Thus, the requirements on vacuum, field emission, etc. are fairly well understood.

At present, all polarized electron photocathode sources are operating using DC guns. A relatively long electron pulse is generated to keep the space charge forces low. The gun is then followed by a bunching system designed either to increase the charge that can be put into single bunches of the accelerating rf, or in some cases simply to increase the efficiency of the injection system.

The development of rf guns has been driven primarily by the need for high brightness sources by FELs. However, since an rf gun eliminates the need for a bunching system, it is also a strong candidate for the electron source for any electron accelerator, especially those requiring a train of closely spaced bunches, as is the case for most linear collider designs. In addition, colliders require a very low emittance beam, which is nominally provided by damping rings. Using an rf gun as the source, the requirements for the electron damping ring are greatly loosened.

---

<sup>#</sup> Permanent address: Stanford Linear Accelerator Center

Some injectors being designed for collider test facilities will use an optical rf gun (CTF, TTF). In addition, at KEK an rf gun has been built which could be used on the ATF. These developments, which have occurred without too much regard for the ultimate need for polarized electrons, provide some “independent” indication of the desirability of an rf gun for colliders.

With the development of rf guns, GaAs was rejected as the cathode material for several reasons, the principal one being that the activated surface of GaAs crystals is too sensitive to the relatively poor vacuum environment of rf guns[2],[3]. At the 8th Int. Symp. on H.E. Spin Physics, 12-17 Sept. 1988, held in Minneapolis, MI, one of the present authors[4] suggested the need to solve this problem and develop an rf gun capable of producing polarized electrons. The first published proposals for using an rf gun with a GaAs cathode for producing electrons were made at the *Workshop on High Intensity Electron Sources*, Legnaro, IT, May 24-28, 1993[5],[6]. Producing *polarized* electrons was the motivating factor for the proposal of ref. [5].

## 2. Prospects and problems for rf guns for polarized electrons

### 2.1. *Space charge limit*

For any electron gun, the space charge limit is determined by the geometry of the gun. For a thermionic cathode or a non-semiconductor photocathode, the space charge limit is observed for a given cathode bias,  $V$ , when there is no longer any increase in the electron current as the cathode temperature or the laser intensity respectively is increased. For DC or long pulsed beams, the space charge limit is really a limit of the current density,  $j$ , and is given by the Child-Langmuir Law[7]:

$$j = kV^{3/2}.$$

For two plane parallel electrodes of infinite extent, the maximum charge that can be extracted in an electron pulse whose duration is less than the transit time of the electrons between the two electrodes is given by Gauss' Law[8]:

$$s = e_o E = 0.885E \frac{nC}{cm^2},$$

where  $E$  is in units of MV/m. Since it is critical for a GaAs cathode that there be no backward accelerated charge, an rf gun for polarized electrons must use a pulse that is short relative to the rf period, thus it will approximate these conditions. For an S-band gun, for which the accelerating field is typically  $\sim 50$  MV/m[9], the space charge limit will be approximately

$$s = 44 \frac{nC}{cm^2}.$$

A collider macropulse generally consists of a string of closely-spaced micropulses, each micropulse having a charge on the order of 1 nC. The relation above applies to each micropulse as long as the micropulse spacing is at least one rf period.

To avoid backward acceleration with an S-band gun, the pulse length should be  $\leq 20$  ps, i.e.,  $\leq 1/20$ th of the rf period. Thus the current limit for a given micropulse due to space charge will be on the order of

$$j = 2.2 \frac{kA}{cm^2}.$$

For very short pulses,[10] it is the charge limit, not the current limit, that is important. The cathode area for an S-band rf gun can be up to  $1.1 \text{ cm}^2$  (the cathode area for the CTF Gun 3b), thus the charge limit for an S-band rf gun is clearly much greater than the requirements of any collider source.

It is interesting to note that for an L-band rf gun, since the dimensions scale inversely with the frequency, the absolute charge limit will be larger, since the maximum cathode area that can be used will scale quadratically. As will be seen below, increasing the cathode area has additional, more important benefits.

## 2.2. Cathode charge limit

There is a limit to the rate at which charge can be extracted from semiconductor photocathodes which is different from, and independent of, the space charge limit. This limit is here called the “cathode charge limit”[11], but it will be seen that it is essentially a current limit.

For photoemitters, a high probability of emission of conduction-band, near-thermal electrons into vacuum is achieved when the vacuum level is lowered below the conduction band minimum in the bulk--defining a negative electron affinity (NEA) surface. The vacuum lowering is achieved by a combination of the band bending and the application of alkalis and oxides to the surface. By having an NEA surface, emission of conduction band electrons to vacuum is achieved merely by applying a negative bias to the cathode. To extract the maximum possible number of electrons, the field must be sufficiently large to overcome space charge limitations.

For heavily p-doped semiconductors, the energy bands are bend downwards at the surface. The band bending region is on the order of 10 nm thick. Electrons which are promoted into the conduction band by the absorption of photons, are, unlike the negatively-charged acceptor ions, free to move to the surface, where the majority are trapped in surface states. This surface charge lowers the internal voltage of the band bending region, effectively flattening the bands. Holes can tunnel through the narrow band bending region to neutralize the electron charge at the surface. Thus the band flattening is inherently temporary. The time constant for this discharge process depends on temperature and dopant density, and is typically a few nanoseconds for highly-doped GaAs ( $2 \times 10^{19} \text{ cm}^{-3}$ ), increasing to 10-100 ns for the medium-doped ( $5 \times 10^{18} \text{ cm}^{-3}$ ) crystals used by SLAC.[12]

The effects of the band flattening on the operation of a GaAs photocathode gun producing a cw beam are not observed since the intensities that can normally be achieved using cw lasers are too low. However, the use of high-power pulsed lasers introduces an additional factor. For a sufficiently high photon flux near threshold, the rate at which near-thermal electrons arrive at the surface begins to compete with the discharge rate of the surface electrons. Thus the first electrons arriving at the surface can raise the vacuum level by a significant amount, blocking at least the less energetic of the succeeding electrons. This is the cathode charge limit[13]. It can be observed for an NEA semiconductor photocathode when, for a given cathode bias, the maximum photocurrent that can be achieved by increasing the (near threshold) photon flux is lower than the space charge limit.

The cathode charge limit depends on the rate of arrival of conduction band electrons at the surface as well as the rate of discharge. The characteristic time for the vacuum level to respond to a change in the charge trapped at the surface is thought to be  $<1 \text{ ps}$ [14]. Thus for a short excitation pulse, the “cathode charge limit” sets an upper limit to the charge density that can be extracted. For practical applications, it establishes a current density limit.

The cathode charge limit has been explored at SLAC using two pulses of 2-ns FWHM with variable separation[12]. The first pulse is used to limit the charge from the cathode. The second (probe) pulse is then found to be affected in intensity inversely with separation from the first. In this manner the relaxation time for the cathode charge limit can be measured. For a collider, the relaxation time must be considerably shorter than

the spacing between microbunches or the intensity within the macropulse will vary when operating near the cathode charge limit.

There are several ways to design a gun to raise the level at which the charge or current becomes limited. The dopant density can be increased (which lowers the polarization), the cathode temperature can be increased (which may lower the QE lifetime), and the bias voltage can be increased. This latter effect will be discussed later. For a given charge or current, the level can also be raised, in effect, by increasing the active area of the cathode.

Increasing the dopant density will narrow the band bending region and consequently increase the internal field. In the band bending region, the former increases the probability of the tunneling by thermally injected holes, the latter increases the probability of field emission of holes. However, a high dopant density appears to decrease the polarization of the photoelectrons. Decreasing the polarization is not acceptable for high energy physics applications. Thus one is left with the proposal to increase the dopant density only within the final nanometers of the surface. The practical application of this technique to strain-lattice cathodes awaits development of a method to clean the surface for activation without using high temperature heating (which evaporates the surface layer and/or causes the high-density dopant at the surface to diffuse into the bulk).

The rate at which holes tunnel through the band bending region is related to their thermal energy. Increasing the cathode temperature should enhance this process although to date the effect of temperature on the cathode charge limit has not been measured. In addition, it is noted that measurements at SLAC indicate the QE lifetime of the SLAC cathodes appears to deteriorate as the cathode temperature is raised from  $\sim 0^\circ\text{C}$  to room temperature[15].

Increasing the active area of the cathode is a straight-forward way to minimize the effect of the cathode charge limit. However, the maximum size of the cathode area is limited by the specific gun design. In addition, it is noted that the gun emittance increases with cathode area. Besides lowering the brightness of the beam, a larger emittance will make it more difficult to prevent beam interception at the anode and downstream by the vacuum system boundaries. Beam interception causes desorption of molecules which can poison the GaAs surface. For the SLAC DC gun, the beam interception in the first meter after the gun is maintained below 0.1%. Thus a very careful study of the beam dynamics using computer simulations must be made to determine the maximum cathode size for an rf gun using a GaAs cathode.

### *2.3. Parameters affecting the cathode charge limit*

For a given temperature and bias voltage, the cathode charge limit has been shown to depend primarily on the surface escape probability,  $\Pi$ [1]. From one crystal to another, a great deal of variety is seen in the measured values of  $\Pi$ . The largest factor is the manufacturer. The strained-lattice GaAs-GaAsP crystals are grown by MOCVD. The exact parameters used by a manufacturer for a given crystal growth are proprietary. However, even for a single manufacturer, the resulting values of  $\Pi$  can vary greatly.

For a given crystal to be used in a given gun system, the final value of  $\Pi$  depends on the cathode preparation technique and on the cathode bias. The evidence for the value of  $\Pi$  achieved is the measured QE.

With a load-lock system, the cathode surface preparation techniques normally used can now produce a fairly standard result.

The cathode bias is known to affect  $\Pi$  (Schottky effect). Using the 2-ns SLC laser pulse, the cathode charge limit for a give QE has been shown to scale with the cathode bias. Thus operating at a higher cathode bias would increase the charge limit. Unfortunately, the SLC experience is that a higher bias generally increases the dark current which in turn lowers the QE lifetime. One alternative is to use a pulsed bias, which would greatly reduce the integrated field emission, allowing a higher operating voltage. Another alternative, actively being explored at SLAC, is to eliminate dust-like particles (thought to be a major source of field emission[16]) from

the gun high-voltage parts by rinsing with high-purity water[17],[18][19] and then to assemble the gun in a dust-free environment. (The latter step is already in effect at SLAC.) See also Section 4.

At first it would appear that the extremely-high cathode voltages associated with an rf gun would also raise the cathode charge limit. As shown below, this may not be the case at all.

#### *2.4. Effect of high electric field on the cathode charge limit*

The SLC gun produces ~10 nC in a 2-ns pulse (~5 A) from a 1.5 cm<sup>2</sup> cathode (~3 A cm<sup>-2</sup>). With the 100-nm, medium-doped strained-layer cathodes presently used, this is nearly the cathode charge limit even when the QE is maximum (i.e., just after activation) and at the operating bias of -120 kV (corresponding to an accelerating voltage at the cathode of 1.8 MV/m).

For an S-band rf gun, a surface accelerating voltage of 50 MV/m is about 30 times higher than that of the SLC DC gun. Thus one would expect the cathode current-density limit to be ~90 A cm<sup>-2</sup>. (This is the most optimistic value possible; no measurement has yet been made.)

On the other hand, since the pulse duration for the S-band rf gun is 100 times shorter than for the SLC pulse, the current necessary to achieve the required SLC charge would be 500 A (300 A cm<sup>-2</sup>)! Fortunately, some collider designs, including NLC/JLC and CLIC, require less charge per bunch than the present SLC operating charge. Thus the current requirement in an rf gun for the present collider plans is ≤160 A. Since, as mentioned earlier, the cathode area of an S-band gun can be up to 2.5 cm<sup>2</sup>, the required current density is <65 A cm<sup>-2</sup>, well below the cathode current limit.

As noted earlier, the maximum possible cathode area for an rf gun varies quadratically and inversely with frequency, while the maximum accelerating field (and thus the cathode current density limit) varies only linearly and inversely. Thus an L-band gun, for which the space charge limit is still quite high, presents a larger ratio of cathode current-density limit to collider current-density requirements than an S-band gun.

#### *2.5. Potential problems affecting operation of a GaAs cathode in an rf gun*

There are two classic problems associated with using GaAs in an rf gun:[2] 1) the time response of the photoelectrons; and 2) the vacuum conditions in an operating rf gun. In addition, the lifetime of the photocathode in the presence of possible rf surface currents and in the presence of ions desorbed by the stray electrons generated by RF breakdown and field emission must be determined.

The photoemission time response has been studied experimentally for several years now by a Legnaro-BINP collaboration. In their latest publication[20], they place an upper limit of ~40 ps on the emission time from bulk GaAs cathode with a QE<1%. In addition, there are grounds for believing that the response time for a very thin photocathode (the SLAC high-polarization strained-lattice cathodes have a epi-layer of GaAs only 100 nm thick) will be <10 ps.[5]

There are several unknown factors for operating an rf cavity which includes a significant volume of semiconductor: 1) the shift in the resonant frequency of the cavity when the semiconductor is introduced (this is not a fundamental problem); 2) the HV breakdown and level of field emission when the semiconductor is introduced--factors to which GaAs photocathodes are very sensitive; and 3) the influence on the cavity operation of possible contamination by the semiconductor material, the surface activation elements (Cs and an oxide), or the materials used to support or "glue" the crystal to the cavity wall.

There has been a great deal of progress reducing RF breakdown and field emission in superconducting rf cavities that is applicable to a polarized rf gun. This work has led to a significant increase in accelerating

gradient in the cavities built for CEBAF and in study for other applications. A derivative of this work has been the impressive results achieved at KEK with a normal conducting (Cu) S-band cavity rinsed with high-purity high-pressure water in clean-room conditions[19].

An upper limit of 50 nA average dark current has been established in the SLAC DC source,[1] above which the QE lifetime of the GaAs cathode begins to visibly diminish when the HV is on. It is not clear how to apply this limit to an rf gun since the desorbed ions, which are presumably responsible for the lifetime effect, will not behave in an rf field the same as in a DC field. Nonetheless, one can measure the dark current generated by an rf gun during the rf pulse and then calculate the average dark current to be associated with any rf duty factor (pulse repetition rate times pulse width) for the same gun at the same field value.

There are technical problems whose solution is not immediately obvious: how to mount the photocathodes on the gun “rf plug”, how to activate the surface of the GaAs crystal, especially if *in situ* heat cleaning cannot be used[21]. How to monitor the gun performance, in particular, how to monitor the “internal” field emission (field emitted electrons that are reabsorbed before leaving the cavity).

### 3. Properties of GaAs

#### 3.1. *General properties*

The general properties of GaAs as found in the literature are summarized in Table 1.

Table 1. General properties of GaAs.[22]

Atoms cm <sup>-3</sup>	4.42x10 <sup>22</sup>
Atomic weight	144.63
Breakdown field	40 MV/m
Crystal structure	Zincblende
Density	5.32 g cm <sup>-3</sup>
Effective mass at 300 K [23]:	
Electrons, m <sub>n</sub> (Γ)	0.063 m <sub>o</sub>
Heavy holes, m <sub>p,h</sub>	0.50 m <sub>o</sub>
Light holes, m <sub>p,l</sub>	0.076 m <sub>o</sub>
Electron affinity	4.07 eV
Energy gap at 300 K	1.424 eV
Intrinsic carrier concentration	1.79x10 <sup>6</sup> cm <sup>-3</sup>
Lattice constant	5.653 Å
Linear coefficient of thermal expansion	6.86x10 <sup>-6</sup> °C <sup>-1</sup>
Melting point	1238 °C

#### 3.2. *Conductivity of GaAs*

Since we are interested in using GaAs in a normal conducting (Cu) rf cavity operating at 3 GHz, it will be useful to calculate the expected conductivity and dielectric strength of GaAs. We first estimate the DC conductivity based on the dopant density of a bulk GaAs crystal of 5x10<sup>18</sup> cm<sup>-3</sup>. The general expression for the conductivity of a semiconductor is given by:

$$\sigma = n e \mu_e + p e \mu_h,$$

where n (p) is the density of electron (hole) carriers, and  $\mu$  is the corresponding mobility.

The minimum conductivity is for intrinsic GaAs, for which  $n=p=n_i$ :

$$\sigma_{\min} = n_i e (\mu_e + \mu_h),$$

where  $n_i \sim 2 \times 10^6 \text{ cm}^{-3}$ ,  $\mu_e = 9.2 \times 10^3 \text{ cm}^2/\text{V-s}$  @ 300 K, and  $\mu_h = 400 \text{ cm}^2/\text{V-s}$  @ 300 K.

Therefore,  $\sigma_{\min} = 3.07 \times 10^{-7} \Omega^{-1}\text{-m}^{-1}$ .

For p-doping of  $5 \times 10^{18} \text{ cm}^{-3}$ ,  $p=5 \times 10^{18} \text{ cm}^{-3}$  ( $N_a \gg N_d$ ),  $n = n_i^2/(N_a - N_d) \sim 10^{-6} \text{ cm}^{-3}$ , and therefore  $\sigma = 3.2 \times 10^4 \Omega^{-1}\text{-m}^{-1}$ .

### 3.3. Dielectric strength of GaAs

The complex dielectric constant[24] is given by

$$\epsilon = \epsilon' - i\epsilon'' = \epsilon_r \epsilon_o,$$

where

$$\epsilon = \epsilon'_r - i\epsilon''_r.$$

A simple model of the atomic contribution to  $\epsilon_r$  has been used by Jackson[25] to derive an expression for  $\epsilon_r$  that is valid for low frequencies. Expressed in MKSA units, the resulting relation is

$$\epsilon_r(\omega) = \epsilon'_r(0) + i \frac{S(\omega)}{\epsilon_o \omega}, \quad (1)$$

where the complex conductivity is

$$S(\omega) = \frac{\epsilon_o f_o g_o \omega_p^2}{(g_o^2 + \omega^2)} + i \frac{\epsilon_o f_o \omega \omega_p^2}{(g_o^2 + \omega^2)}. \quad (2)$$

In eq. (2),  $\omega_p$  is the plasma frequency given by

$$\omega_p = \left( \frac{Ne^2}{m\epsilon_o} \right)^{1/2}. \quad (3)$$

The dependency on N, the number of electrons per unit volume, is contained in  $\omega_p$  and the damping constant (otherwise known as the effective collision frequency),  $\gamma_o/f_o$ , where  $f_o$  is the fraction of electrons that are “free” in the sense that the restoring force,  $\vec{F}$ , for a charged particle of mass m oscillating with frequency  $\omega_o$  about equilibrium,  $\vec{F} = -m\omega_o^2 \vec{x}$ , is zero. The contribution of all the other charged particles is contained in  $\epsilon'_r(0)$ .

Note that if  $\omega \ll \gamma_0$ ,  $\sigma(\omega)$  is real with a ; by contrast,  $\epsilon_r(\omega)$  retains an imaginary part (albeit generally small). In addition note that the real part of  $\epsilon_r(\omega)$  contains a term from  $\sigma(\omega)$  as well as  $\epsilon_r'(0)$ .

Following Jackson[25], if  $\omega \ll \gamma_0$ , the ratio  $\gamma_0/f_0$  can be calculated from equation (2) above by using a known value of  $\sigma$ :

$$\frac{g_o}{f_o} \approx \frac{e_o W_p^2}{S}. \quad (4)$$

Note that in equations (1) to (4), the dimensions for  $\omega$ ,  $\gamma_0$ , and  $\omega_p$  are  $s^{-1}$ , for  $\sigma$  the dimensions are  $\Omega^{-1} m^{-1}$ , while  $\epsilon_r$ ,  $\epsilon_r'$ , and  $f_0$  are dimensionless.

In Table 2, the calculated values of  $\omega_p$  and  $\gamma_0$  for Cu and GaAs are shown. For GaAs, the effective mass of heavy holes,  $m_{p,h}$ , is used for  $m$ . The measured value of  $\sigma$  for Cu at room temperature and at low frequency is taken from Table 3. The value of  $\sigma$  for GaAs is calculated in Section 3.2 above. Finally,  $f_0$  is assumed to equal 1.

Table 2. Calculated values of some constants for Cu and GaAs.

Parameter	Cu	GaAs/p= $5 \times 10^{18} \text{ cm}^{-3}$	GaAs (intrinsic)
$\omega_p$ (Hz)	$1.6 \times 10^{16}$	$1.8 \times 10^{14}$	$8 \times 10^7$
$\gamma_0$ (Hz) <sup>(a)</sup>	$4 \times 10^{13}$	$8.9 \times 10^{12}$	$1.9 \times 10^{11}$
$\left(\frac{W_p}{g_o}\right)^2$	$1.6 \times 10^5$	818	~0
$\frac{S}{e'w}$ (a)	$10^3$	$10^2$	$10^{-7}$
Notes:			
(a) Calculation valid only for $\omega \ll \gamma_0$ .			

From eqs. (1) and (2), if  $\omega \ll \gamma_0$ , one can see that

$$\epsilon_r'(\omega) \approx \left( \epsilon_r'(0) - \frac{f_o W_p^2}{g_o^2} \right).$$

The ratio  $\left(\frac{W_p}{g_o}\right)^2$  is given in Table 2, and the corresponding value of  $\epsilon'_r$  in Table 3. Note that for high-N (metallic) materials,  $\epsilon'_r \ll 0$  for  $\omega \ll \gamma_o$ , characteristic of anomalous dispersion, while  $\epsilon''_r \gg 0$ , which in a region of anomalous dispersion indicates dissipation of energy from the electromagnetic wave into the medium. See Section 3.4 below. The corresponding values of  $\sigma$  remain real and positive over all values of N.

### 3.4 Skin depth

Again following Jackson [25], if the fields are assumed to vary in space and time as  $e^{i\vec{k}\cdot\vec{x}-i\omega t}$ , then the wave number, k, is given by the complex expression

$$k = (m\epsilon)^{1/2}\omega = (m\epsilon\epsilon_o)^{1/2}\omega. \quad (5)$$

Substituting eq. (1) for  $\epsilon_r$ , one has

$$k^2 = m\epsilon'\omega^2 \left(1 + i\frac{S}{\epsilon'\omega}\right),$$

where  $\epsilon' = \epsilon'_r\epsilon_o$ . The square root can be expressed as

$$k = b + i\frac{a}{2}, \quad (6)$$

where

$$r = \sqrt{m\epsilon'}\omega \left[ \frac{\sqrt{1 + \left(\frac{S}{\epsilon'\omega}\right)^2} \pm 1}{2} \right]^{1/2},$$

letting  $\rho$  represent  $\beta$  ( $\alpha/2$ ) for the upper (lower) sign.

Using eq. (6), it is seen that waves propagate in a conducting medium as

$$\vec{X} = \vec{X}_o e^{-\left(\frac{\alpha}{2}\vec{n}\cdot\vec{z}\right)} e^{i\vec{n}\cdot\vec{x}-i\omega t},$$

where  $\vec{X}$  is either  $\vec{E}$  or  $\vec{H}$ , and  $\alpha$  is thus clearly the attenuation constant.

A good conductor is characterized by  $\frac{S}{\epsilon'\omega} \gg 1$ . In this case,

$$b = \frac{a}{2} = \left( \frac{mws}{2} \right)^{\frac{1}{2}} = \frac{1}{d_s}, \quad (7)$$

where  $\delta_s$  is the skin depth. We tabulate  $\frac{S}{e'w}$  in Table 2, while  $\delta_s$  is shown in Table 3.

Table 3. Comparison of Properties.

	$N^{(a)}$ ( $\text{cm}^{-3}$ )	Relative dielectric strength, $e'_r$	Conductivity $\sigma$ ( $\Omega^{-1}\text{-m}^{-1}$ ) @300 K	Skin depth[§3.4] $\delta$ ( $\mu\text{m}$ ) @3 GHz
Alumina		4.5-8.4@1 MHz	$3 \times 10^{-12}$ [26]	
GaAs (intrinsic)	$2 \times 10^6$	13.1[23],[27] for $v \ll 100\text{MHz}$	$2 \times 10^{-7}$ [23] $3.1 \times 10^{-7}$ [§3.2]	
GaAs/p	$5 \times 10^{18}$	-800@3GHz [§3.3]	$3.2 \times 10^4$ [§3.2]	51.5
Mo			$1.8 \times 10^7$ [26]	2.1
Cu	$8 \times 10^{22}$	$-10^5$ @3GHz [§3.3]	$5.8 \times 10^7$ [26]	1.2
Notes:				
(a) N is the number of free electrons (holes) per $\text{cm}^3$ with 1 free electron (hole) per (doping) atom assumed.				

### 3.5. Relation between electrical and optical properties

It is interesting to relate the expressions used for optical properties of materials[28] with those derived above.

The complex index of refraction,  $n$ , is given by

$$n = h - ik, \quad (8)$$

where the real part of the index is  $h$ , and the extinction coefficient,  $k$ , is the imaginary part. Since the index of refraction is related to the dielectric strength by

$$n^2 = h^2 - k^2 - i2hk \equiv e_r = e'_r - ie''_r, \quad (9)$$

it is easy to show with eqs. (5) and (6) with (8) that  $k$  is directly related to the absorption coefficient (earlier called the attenuation constant) by

$$a = \frac{4pk}{|},$$

where  $|$  is the wavelength of the incident radiation.



At SLAC, two bulk-grown GaAs crystals, doped to  $5 \times 10^{18} \text{ cm}^{-3}$ , were cut roughly in a circle of diameter 12 mm from a 356  $\mu\text{m}$  thick wafer. Two Mo plugs similar in shape to the tip of the Cu plugs used to support the  $\text{Cs}_2\text{Te}$  cathodes for the CTF rf gun were prepared at CERN and sent to SLAC. At SLAC, a step was machined in the face of each plug to recess the GaAs crystal to be flush with the surface. See Fig. 2. The exposed surface of the Mo was then cleaned, diamond-paste polished to a 1- $\mu\text{m}$  finish, chemically cleaned one final time, then fired. The crystal was attached to the Mo plug in vacuum using In as a *glue*, as is commonly done in industry, i.e., for mounting substrates for MBE growth. Two crystal-plug assemblies were prepared. Sample 1 was the *test* sample. It underwent several experimental gluings to perfect the technique. Sample 2, which was glued last and only once, was of slightly better quality, meaning the surface finish of the Mo was somewhat better and the In in the Mo-crystal joint that faces the rf cavity was somewhat smoother.

The melting point of indium at atmospheric pressure is 156.6°C, so it was out of the question to heat clean these samples in the normal manner.

At CERN, Samples 1 and 2 were designated in the Photoemission Lab as Cathodes 45 and 46 respectively. The cathodes were cleaned with ethanol and ultrasonic rinsing, then installed in the cathode transport apparatus. The transporter[30] was then baked at 120°C for 48 hours. At first the outgassing was quite bad, but the final pressure, about  $2 \times 10^{-10}$  Torr, was not much higher than is normal for baking  $\text{Cs}_2\text{Te}$  cathodes.

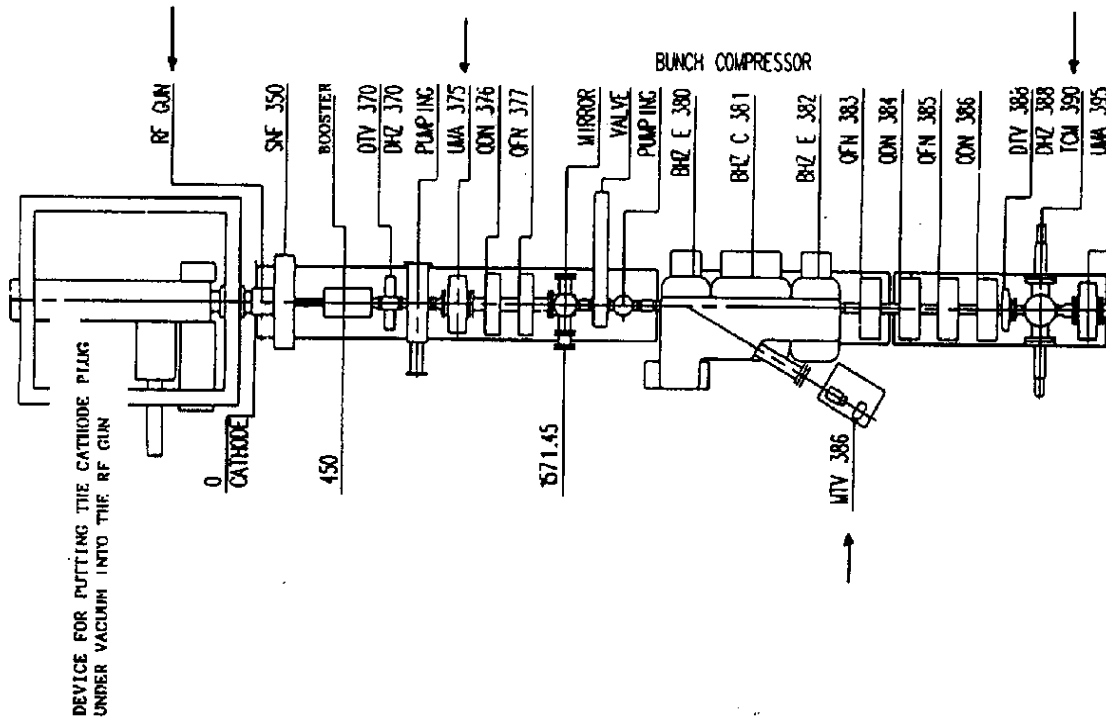


Fig. 3. Layout of components in CTF-1.

Next the samples were each installed in the 1.5 cell rf gun (Gun 3b) in CTF-1 for low power rf tests. The layout of components in CTF-1 is shown in Fig. 3. An HP 8753B network analyzer was connected to the rf input of the gun to measure the frequency shift due to the GaAs plus Mo. The cavities had been tuned for the

solid Cu plugs that are used for the Cs<sub>2</sub>Te cathodes.[31] The nominal tuning range for the gun is ±1 MHz. The results of the frequency measurements are shown in Table 4.

Table 4. Low power frequency measurements in RF Gun 3b in the order performed.

Cathode	Measured frequency (GHz)	Comments
Cs <sub>2</sub> Te	2.99851	Starting condition
GaAs 1	2.99845	
GaAs 2	2.99862	
Cs <sub>2</sub> Te	2.99859	Original Cu plug reinstalled

From Table 4 it can be seen that the frequency shift due to installing the GaAs samples (30-110 kHz) was similar to that for simply reinstalling the same plug (80 kHz). The predicted frequency shift for the exchange of Cu by the GaAs crystal is ~100 Hz (see Section 4.2), which is much, much smaller than the frequency shift observed here when reseating a plug.

The tuning sensitivity for the GaAs samples has been calculated to be 1.7 kHz/μm (see Section 4.2). Allowing 80±40 μm for the repeatability of seating the plugs, it appears the two GaAs samples are accurately dimensioned to <20 μm, where this limit is dominated by the accuracy expected for the repeatability of the seating.

#### 4.2. Expected shift in the frequency of the 1.5-Cell CTF Gun 3b due to the introduction of a dielectric cathode

One can calculate the expected shift in frequency from the Slater Perturbation Theorem:[32]

$$\omega^2 = \omega_o^2 \left[ 1 + k \frac{\Delta t}{2U} \int (\overline{m\vec{H}_1^2} - \overline{e_1\vec{E}_1^2}) dt \right], \quad (10)$$

where  $\omega_o$  is the unperturbed frequency of the gun,  $\Delta t$  is an element of the perturbing volume, and  $U$  is the average rf energy stored in the 1.5 cell gun. For small perturbations,

$$d = \frac{\omega - \omega_o}{\omega_o} = \frac{k \int (\overline{m\vec{H}_o^2} - \overline{e_1\vec{E}_o^2}) dt}{4U}. \quad (11)$$

Since  $U = \omega_o QW$ , where  $\omega_o = 2\pi f_o$ ,  $f_o = 3 \times 10^9$  Hz,  $Q = 11000$  for the 1.5 cells,[33] and  $W = \text{power loss} = 7$  MW (max.), then  $U_{\text{max}} = 4.0$  J.

In our case, the 1/2 cell operates in the E010 mode. Although the conductivity of the highly-doped GaAs is less than that of Cu (see Table 3), the cathode is located in an area where  $\vec{H} \sim 0$  and  $\vec{E}$  is perpendicular to the surface. Thus the resistivity of the cathode is expected to have little effect on the Q of the cavity.

With the network analyzer, it was seen that the bandwidth of the cavity was not broadened by the presence of the GaAs crystal, confirming the conclusion that the cathode conductivity is not important in this case.

Since  $\vec{H}_1 \rightarrow 0$ ,  $k \rightarrow 1$ , and  $\vec{E}_1 \sim \text{constant}$ ,  $d = \frac{-e_1 E_1^2 V_1}{4U}$ , where  $V_1$  is the perturbing volume, and  $E_1 = \frac{E_o}{e_{r1}}$ ,

where  $E_o$  is the field in the unperturbed cavity and  $e_{r1} = \frac{e_1}{e_o}$ . For this experiment, the cathode is mounted in

the step shown in Fig. 2 that is machined in the Mo cathode plug such that the surface of the GaAs crystal is flush with the Cu wall of the cavity. The cylindrical cathode of radius  $r$  and height  $h$  has a volume of  $V_1 = \rho r^2 h$ . Therefore

$$d = -e_o \frac{E_o^2 \rho r^2 h}{e_{r1} 4U}. \quad (12)$$

It should be noted that eqs. (10) and (11) above are a simplification of the general case of a cavity in which the perturbation replaces one material of volume and permittivity  $V_i$  and  $\epsilon_i$  with that of  $V_f$  and  $\epsilon_f$ . Thus eq. (12) can be generalized to:

$$d = -e_o \frac{E_o^2 \rho}{4U} \left( \frac{V_f}{e_{rf}} - \frac{V_i}{e_{ri}} \right). \quad (13)$$

For our case,  $r_f = r_i$ . However, the height of the perturbation volume,  $h$ , is limited by the lack of penetration of the rf field. If we use the skin depth,  $\delta_s$ , from Table 3, as a measure of the penetration of the field, then eq. (13) becomes:

$$d = -e_o \frac{E_o^2 \rho r^2}{4U} \left( \frac{d_{sf}}{e_{rf}} - \frac{d_{si}}{e_{ri}} \right). \quad (14)$$

The significance of the negative sign for  $\delta$  is that if  $\frac{d_{sf}}{e_{rf}} > \frac{d_{si}}{e_{ri}}$ , the frequency should decrease. This is

equivalent to saying the frequency should decrease if the perturbation volume increases. One can think of all perturbations as an exchange of two materials. For a Cu tuner, if the tuner is moved so as to reduce the vacuum volume of the cavity by  $V_i$ , then one can think of this as replacing a vacuum volume of  $\frac{V_i}{e_{ri}}$ , where  $\epsilon_{ri} = 1$ , with

a Cu volume of  $\frac{V_f}{e_{rf}}$ , where  $\epsilon_{rf} \approx 10^5$  (see Table 3). Note that because of limits on the penetration of the field

into Cu,  $V_f \ll V_i$ . Thus the frequency should increase.

For our test, in which Cu is replaced by highly-doped GaAs,  $E_o = 100$  MV/m (max.),  $r = 6$  mm,  $h_i = \delta_{oi} = 1$   $\mu$ m,  $\epsilon_{ri} \approx -\infty$ ,  $h_f = \delta_{sf} = 50$  mm, and  $\epsilon_{rf} \approx -800$ . Thus, using eq. (14):

$$d = -8.8 \times 10^{-12} \frac{(10^8)^2 \rho (6 \times 10^{-3})^2}{4(4)} \left( \frac{50}{-800} - \frac{1}{-10^5} \right) 10^{-6} = 3.9 \times 10^{-7}.$$

Since  $\Delta f = df_0$ ,  $\Delta f \sim 100$  Hz.[34]

The permittivity of highly-doped GaAs is large enough that it appears to the rf cavity to be just like Cu. If either the highly-doped GaAs crystal or Cu the same size as the crystal were to be placed in the cavity at the cathode location, replacing vacuum volume, the frequency shift would be 600 kHz. This is equivalent to a detuning sensitivity of  $\frac{\Delta f}{\Delta h} = 1.68$  kHz/ $\mu\text{m}$  for either a Cu or a GaAs tuner of diameter 12 mm.

#### 4.3. Initial measurements in DC gun

Following the low power rf tests, the transporter with the GaAs samples was returned to the Photoemission Lab for DC gun tests. The DC gun was cleaned and baked in preparation for these tests.

The dark current from the DC gun was measured about a meter downstream of the gun using a Faraday cup and a picoammeter. The detection threshold was several picoamperes.

Each sample was first installed in the gun without being cesiated. The gun bias was provided by a 100-kV DC power supply. The cathode-anode gap was 1 cm. The cathode bias was increased until the maximum available DC field at the cathode was reached--about 9 MV/m. No dark current was observed, just as for Cs<sub>2</sub>Te cathodes.

Sample 2 was then cesiated with a nominal 1.0 nm layer of Cs--approximately 1 monolayer (ML). The Cs layer thickness was estimated by measuring the Cs flow rate using a quartz-crystal thickness monitor and controlling the application time with a shutter. A sticking coefficient of 1 was assumed. The field was increased to as high as 9 MV/m. The dark current behavior in this case was similar to that for no Cs. Going to higher fields was not possible because of high voltage (HV) breakdown.

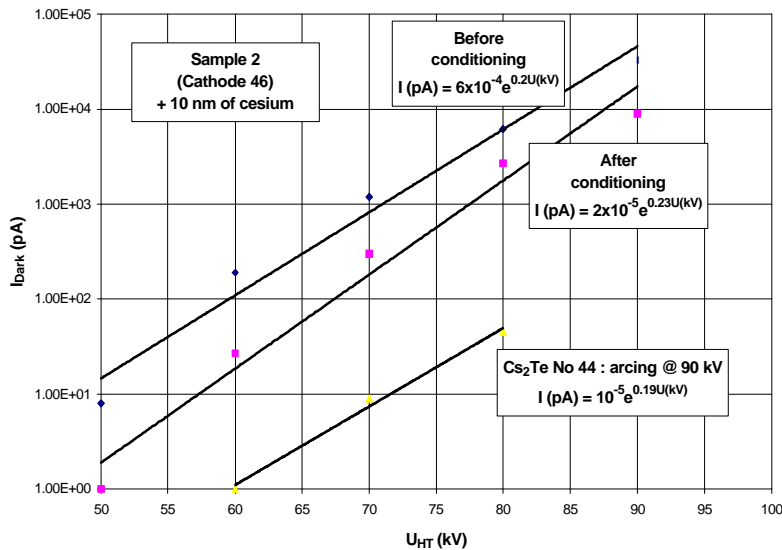


Fig. 4. Dark current in the DC gun for Sample 2 with 10-nm Cs compared to a “bad” Cs<sub>2</sub>Te cathode.

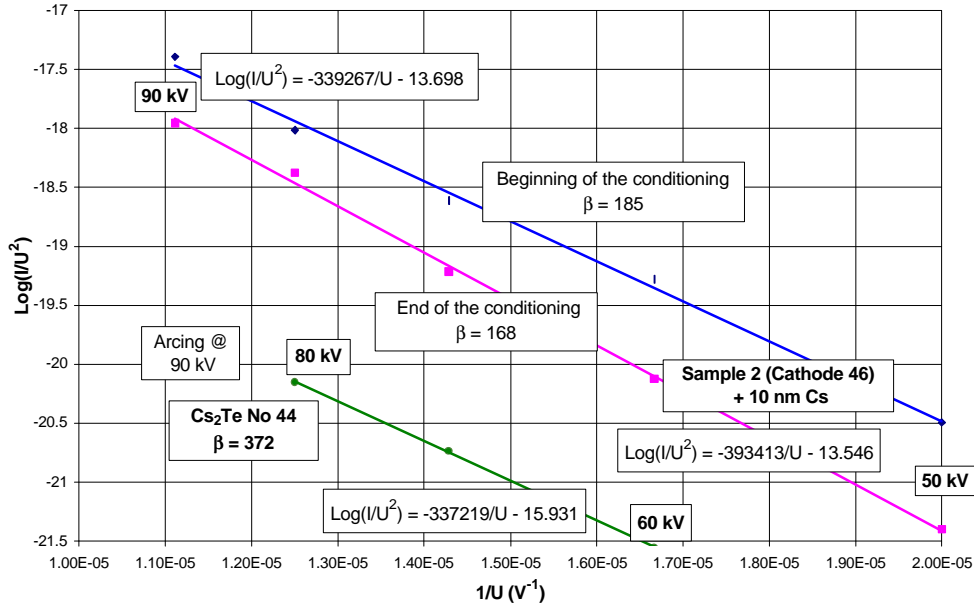


Fig. 5. Fowler-Nordheim plot of same data as in Fig. 4.

Finally, the thickness of Cs on Sample 2 was increased to a nominal 10 nm. (This is probably not much more than 1 ML since the sticking coefficient of Cs is expected to drop rapidly after the first ML.) Dark current for this case was readily observed--initially  $\sim 1$  nA at 7 MV/m and  $\sim 50$  nA at 9 MV/m, reduced by a factor of  $\sim 3$  after conditioning. A comparison of the field emission in the DC gun for this test and a test with a “bad” Cs<sub>2</sub>Te cathode[35] is shown in Fig. 4. The same data is presented in Fig. 5 in a Fowler-Nordheim plot[36] in order to compute the field enhancement factor  $\beta$ . It is interesting that although the dark current for the cesiated GaAs cathode is higher than for the “bad” Cs<sub>2</sub>Te cathode, the  $\beta$  values are lower.

The QE measured in the DC gun is given in Table 5. The green light from a doubled Nd:YAG and the blue light from the same YAG quadrupled was used for these measurements.

Table 5. QE measured in the DC gun.

Sample	Cs layer (nm)	Field (MV/m)	Green (532 nm)	Blue (266 nm)
1, 2	0	9	$<10^{-8}$	
2	1.0	7	$1.5 \times 10^{-8}$	$2.6 \times 10^{-5}$
2	10	7	$3.6 \times 10^{-6}$	$2.6 \times 10^{-3}$
2 <sup>(a)</sup>	10	7	$4.2 \times 10^{-7}$	$1.9 \times 10^{-3}$

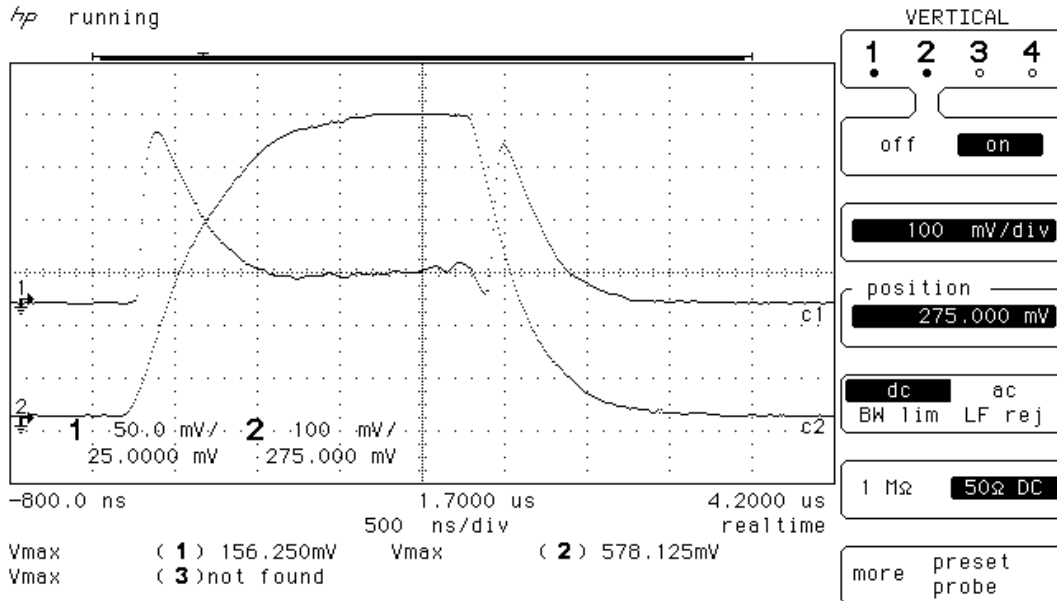
Notes:  
(a) Measured after sample was “stored” under vacuum for 3 days.

The electron affinity (energy difference between the conduction band minimum *at the surface* and the vacuum level) for clean GaAs is 4.07 eV and the band gap at room temperature is 1.42 eV.[22] For a semiconductor, the work function depends on the position of the Fermi level and also, for highly-doped semiconductors, on the band bending at the surface. Thus, in the absence of band bending, the maximum work function of clean GaAs is about 5.4 eV if the Fermi level is pinned to the valence band maximum. For our sample, which is heavily p-doped, the band bending at the surface is expected to be about 0.7 eV, lowering the work function to 4.7 eV. However, for these tests the GaAs surface was certainly not atomically clean before the Cs was applied. Thus an interfacial barrier is assumed to exist that limits the capability of a Cs overlayer to lower the work function. For the thicker Cs layer, one should consider primarily the work function of metallic Cs, which is 2.14 eV.[26] For comparison, the work function of Cs<sub>2</sub>Te is 3.5 eV. When the excitation is with the green light (2.3 eV), the photoemission is almost surely from the Cs layer itself. When blue light (4.7 eV) is used, it is possible that hot (ballistic) electrons from the conduction band of the GaAs make an additional contribution to the photoemission.

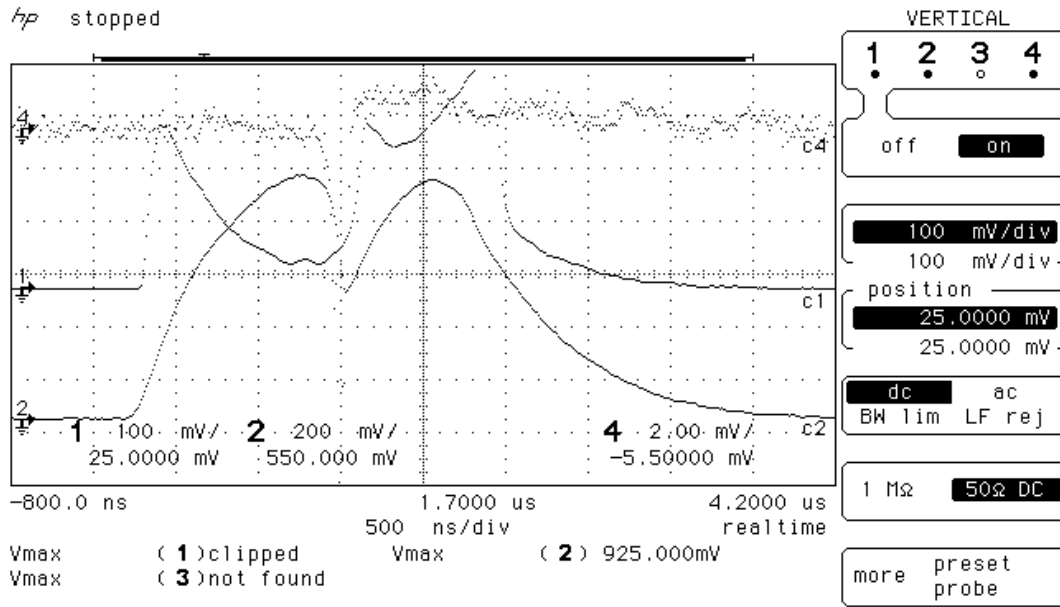
#### 4.4. High power rf measurements

Following the initial tests in the DC gun, the transporter with the GaAs samples was again taken to the CTF-1 and first Sample 1, without Cs, was installed in Gun 3b. The field at the cathode was slowly increased--accompanied by a considerable amount of HV breakdown--over a 12-hour period to a maximum of 87 MV/m. Scope traces of the reflected rf pulse and of the signal from a probe loop, GL2, in the gun are shown in Fig. 6(a) for relatively low rf power and no breakdown. At slightly higher power, a breakdown pulse is shown in Fig. 6(b). The base pressure, which had been  $1 \times 10^{-10}$  Torr before the conditioning began, rose to a maximum of  $1 \times 10^{-8}$  Torr during the conditioning. At the maximum field, no dark current could be detected, but there was visible light on the spectrometer screen. In Section 4.5 following, it is shown that the upper limit of the dark current was  $\sim 60$  pC/( $\mu$ s of rf). This can be compared with 2 nC/( $\mu$ s of rf) measured in an L-band rf gun operating with a field at the cathode of 26 MV/m.[37]

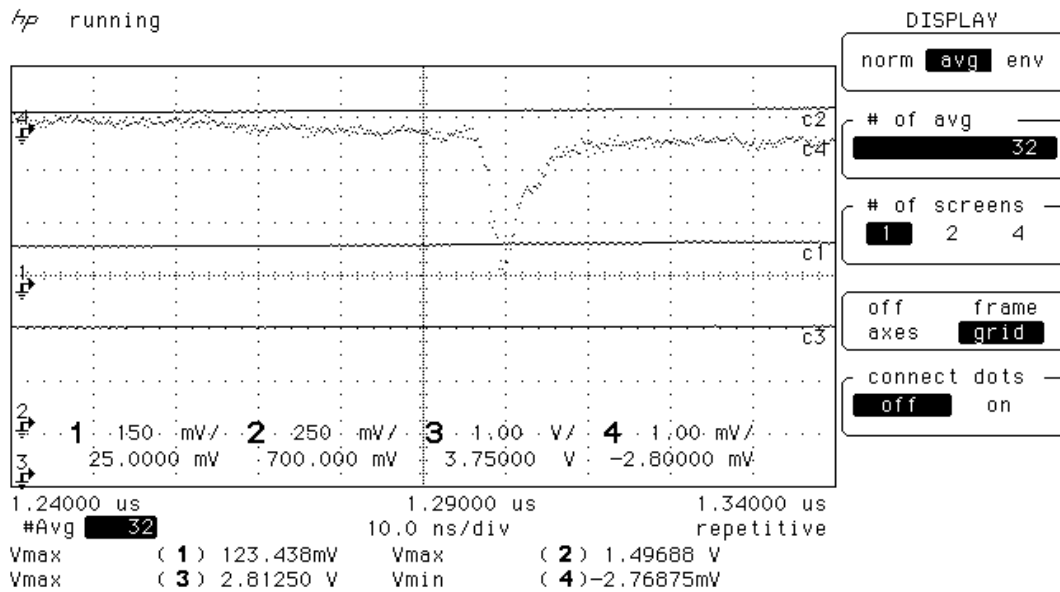
Fig. 6. Scope traces for Sample 1: Curve no. (1) is the reflected rf power signal. The continuously noise in the reflected rf signal could be caused by multipactoring. Curve no. (2) is the signal from the probe loop, GL2, which is in the full cell of the rf gun. The field on the cathode [MV/m] is given by the peak value for curve no. (2) [V] times 46.1. Curve no. (4) is the sum signal from UMA 375, for which the sensitivity is  $\sim 0.7 \times 10^8$  e<sup>-</sup>/mV.



(a) Reflected and probe loop rf signals for 27 MV/m.



(b) RF breakdown for field of 43 MV/m.



(c) Photoemission pulse of  $2 \times 10^8 e^-$  at field of 69 MV/m. Since the laser energy was 260  $\mu\text{J}$ , the corresponding QE was  $6 \times 10^{-7}$ .

The sample was illuminated with blue laser light (262 nm) from a quadrupled Nd:YLF at an energy of 260  $\mu\text{J}$ . The first current monitor downstream of the gun was the sum signal from the position monitor pick-up, UMA 375. The scope trace of the current signal for a field of 69 MV/m is shown in Fig. 6(c). The QE corresponding to this trace is  $\sim 6 \times 10^{-7}$ . For a given field, the gun phase in the cavity had to be re-optimized using the first

spectrometer, BHZ 380 and MTV 386.[38] (See Fig. 3.) The QE measured in this manner is plotted as a function of rf field at the cathode surface in Fig. 7, and a Schottky plot using the same data is shown in Fig. 8. The QE at full voltage was  $\sim 1 \times 10^{-6}$ .

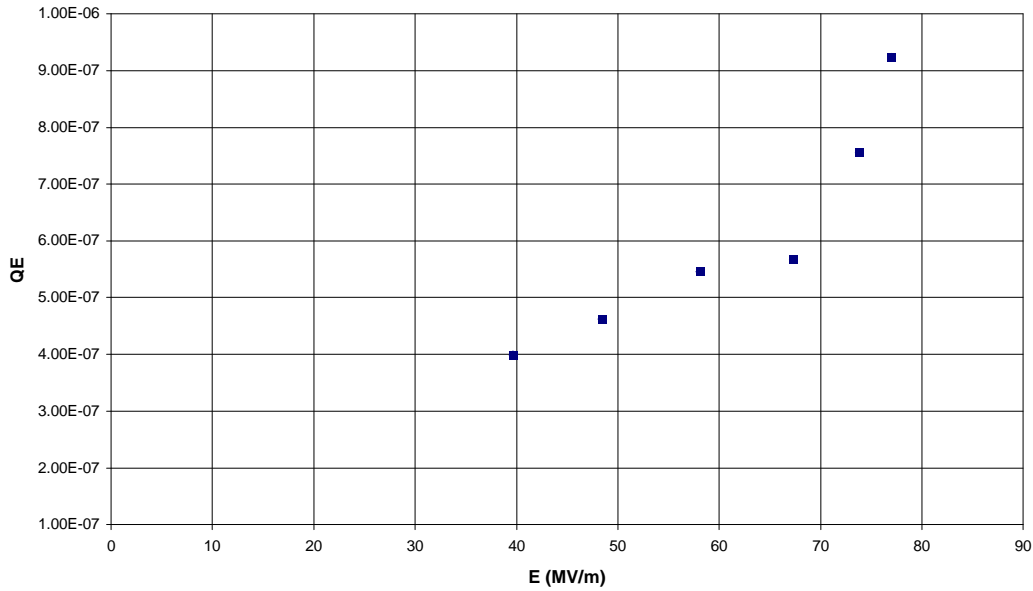


Fig. 7. QE for Sample 1 measured as a function of field at the cathode surface, with the field re-optimized at each setting using a spectrometer.

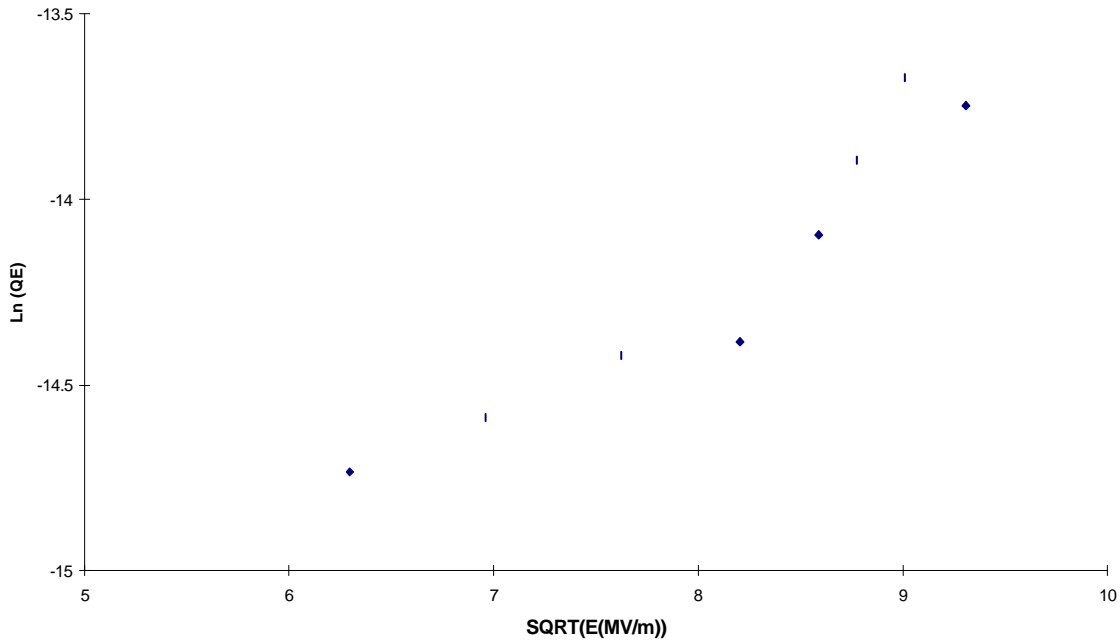


Fig. 8. Schottky plot for same data as in Fig. 7.

The light intensity was varied to ensure the absence of any saturation effects.



Sample 2, for which the GaAs still had a nominal 10-nm layer of Cs, was tested next. It was rf conditioned more gently than Sample 1 over a 6-hour period up to a field of 60 MV/m. This field is just above the level at which multipactoring is excluded ( $\sim 40$  MV/m) in the gun half-cell. For both samples the conditioning became more difficult at this level. During the conditioning, the pressure was mostly below  $1 \times 10^{-9}$  Torr. The number of discharges was considerably less than with Sample 1.

At the top field, when illuminated with 157  $\mu$ J of blue laser (262 nm) light, the photoemitted current was about 1.9 nC, corresponding to a QE of  $\sim 6 \times 10^{-5}$ . See Fig. 9.

At the maximum field, the charge was measured as a function of laser energy. Again no saturation effects were observed. See Fig. 10.

The pulse length of the electron bunch photoemitted with a cathode field of 55 MV/m (maximum value, see ref. [38]) was measured by inserting a thin sapphire radiator, TCM 390, into the 6 MeV beam. See Fig. 3. The resulting Cherenkov light was transported to a streak camera[39] located next to the laser room. The pulse length of the Cherenkov light was measured to be 16 ps FWHH. The length of the laser excitation pulse was 12 ps, measured earlier using the same streak camera. Since the beam energy out of the gun was about half its normal value, this apparent pulse lengthening could have been due to the finite velocity spread in the beam as well as to a slow cathode response photoemission time. The latter case is unlikely here since the photoelectrons are probably all from the surface.

After testing of Sample 2 in the rf gun, no additional analysis was made of the condition of the gun itself.

#### 4.5. Estimate of dark current

The first current monitor downstream of the gun was the position monitor pick-up, UMA 375. The UMAs are wide band pick-ups: 60 kHz to 250 MHz for the sum signal.[40] The sensitivity is 470 mV/A.

In between testing GaAs Samples 1 and 2, the Cs<sub>2</sub>Te cathode was reinstalled and a single-pulse beam produced. On the UMA digital display panel, a pulse intensity of  $47 \times 10^8$  e<sup>-</sup> with laser on was indicated for UMA 375,  $13 \times 10^8$  e<sup>-</sup> with the laser off, or a net pulse intensity of  $34 \times 10^8$  e<sup>-</sup>. The corresponding pulse on the scope was 47.5 mV at the peak with a pulse width of  $\sim 5$  ns if one takes into account the ringing. This corresponds to a sensitivity of 435 mV/A, which is very nearly the 470 mV/A of ref. [40].

The noise of the UMA signal on the scope was about 1 mV. Thus the minimum signal that could have been detected was about 2 mA.

The rf for the gun and booster (generated by MDK98) during the experiment was 1.6  $\mu$ s long at a repetition rate of 10 Hz. Thus the upper limit of the dark current set by UMA 375 was  $\sim 2$  nC/( $\mu$ s of rf).

Dark current was observed on the un-doped alumina screen at MTV 386 in the spectrometer. The light level was quite dim. A very rough calibration of the screen can be had from the experience with the single-bunch beam of 0.5 nC/pulse produced with Sample 2 at  $\sim 45$  MV/m field. This beam on the screen was at least 5 times brighter than the dark current. Thus a reasonable upper limit of the combined (gun and booster) external dark current is 60 pC/( $\mu$ s of rf), a factor of  $\sim 30$  below the measurement of ref. [37].

For an S-band rf gun for the CLIC main beam injector, for which the rf pulse repetition rate will be 1700 Hz, the 50 nA average dark current limit for the SLAC DC gun translates to a required dark current of  $< 30$  pC/( $\mu$ s of rf) at full cathode field (100 MV/m peak?).

With a field at the cathode of only 45 MV/m, the beam exiting the gun plus rf booster is only half its normal momentum. Thus longitudinal space charge forces are expected to be significant. The momentum spread of the beam at normal momentum is about  $\pm 3.5\%$ . [33] The energy acceptance of the spectrometer is  $\pm 6\%$ . [41]

The upper limit measured here does not include the “internal” dark current nor the dark current generated in the following 4-cell rf booster. However, for a clean gun, dark current is not expected from the Cu itself when the rf voltage at the surface is  $< 100$  MV/m (the maximum surface field on the irises in the booster is always  $< 60$  MV/m). Thus the observed dark current was almost surely from the cesiated-GaAs cathode.

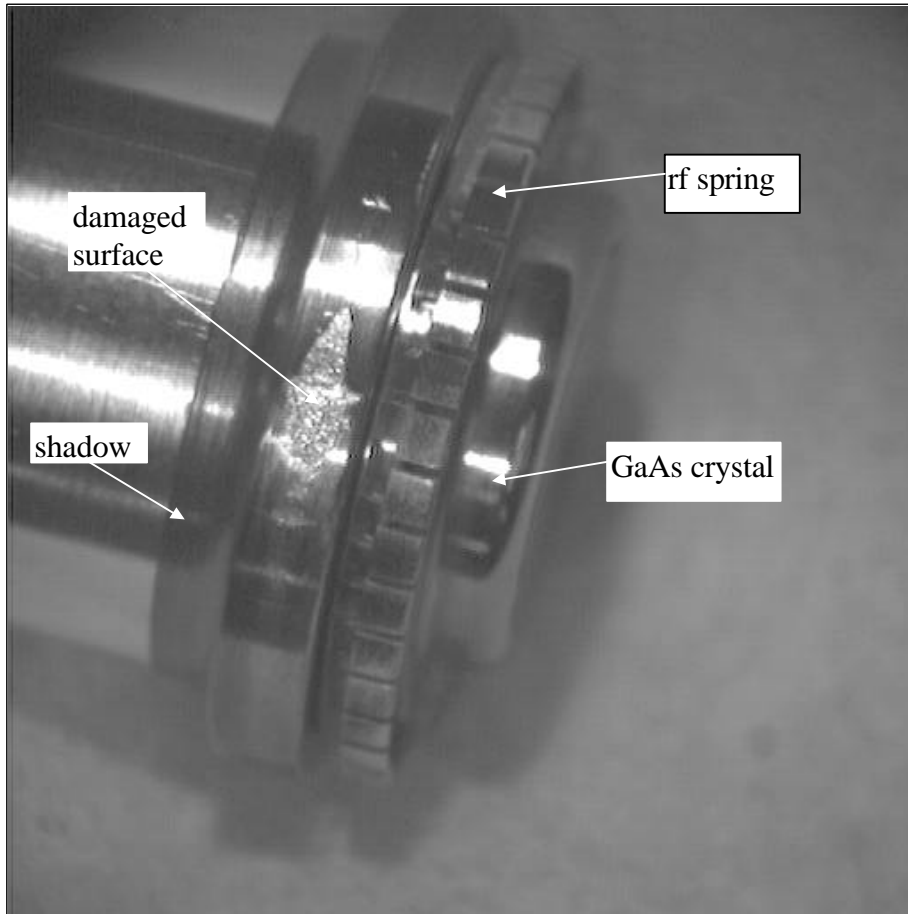


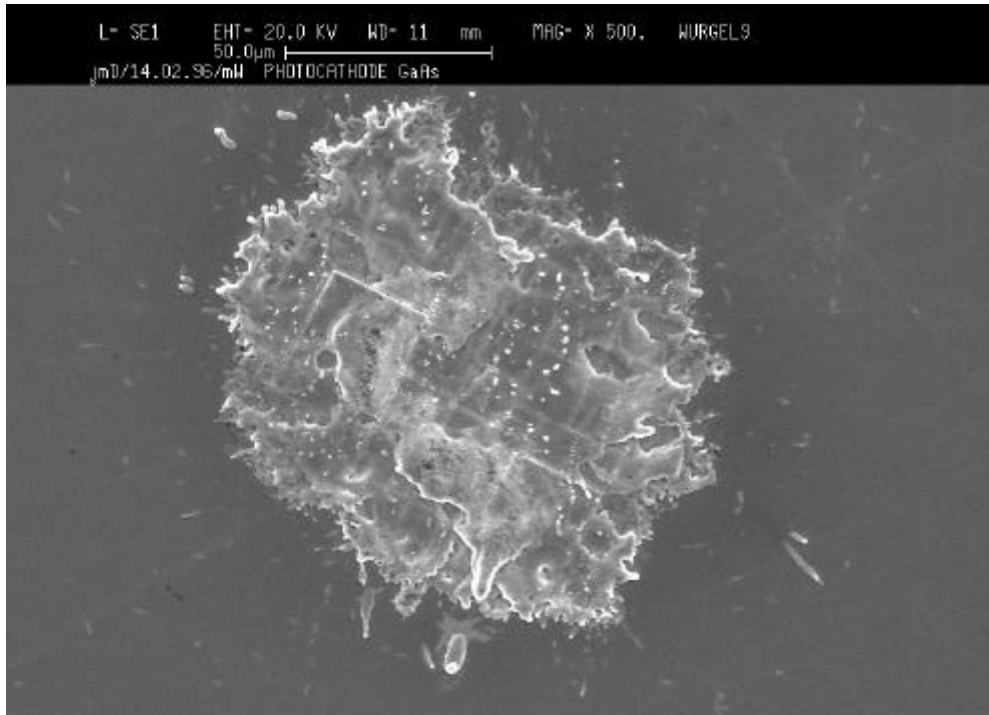
Fig. 11. RF plug for Sample 1 after high-power rf conditioning. The damaged surface is on the raised portion of the Mo nose just behind the rf spring. When comparing this photograph with Fig. 2, allowance must be made for shadows.

For high levels of dark current, it is sometimes possible to observe “internal” dark current by the beam loading on the reflected rf pulse signal. The expected beam loading in Gun 3b for  $1 \mu\text{C}$  is 30%. Thus for 1.9 nC (Fig. 9), the beam loading should be 0.06%. However, as is clear from Fig. 6(a), a 5% mismatch between the gun and the rf window dominates in this case, completely obscuring any beam loading effect.

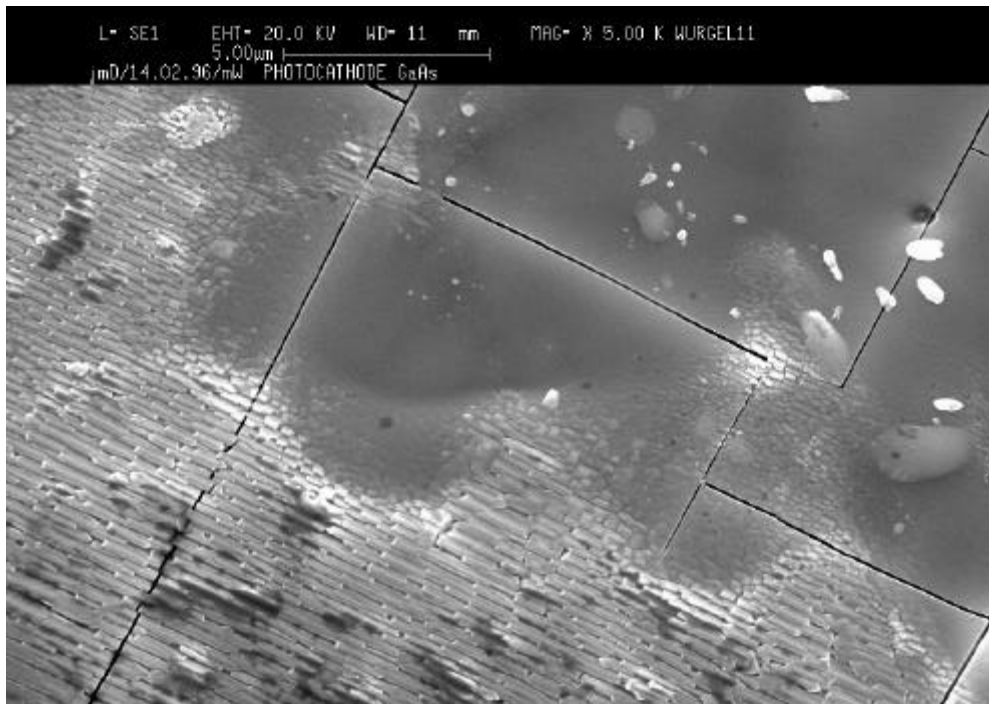
For comparison, the external dark current of Gun 2, measure when new (and relatively dirty) with a Cu plug and a Faraday cup immediately after the gun, was 14 mA in 1.5- $\mu\text{s}$  of rf at 97 MV/m, scaling to  $\sim 0.1$  mA at 45 MV/m or 100 pC/( $\mu\text{s}$  of rf). [33]

Gun 3b was cleaned using the high pressure, ultra-pure water cleaning technique. [18] This may have contributed to the low dark current. [42]

Fig. 12. Electron microscope enlargement of surface speck on Sample 1 after rf conditioning.



(a) Magnification: x500.



(b) Magnification: x5K. Surface cracks and re-crystallization are clearly visible.

#### 4.6. Post-measurement analysis

The two samples were eventually removed from the vacuum system and examined visually. Sample 2 showed no damage. Sample 1 had extensive material deterioration in the area of the rf seal, correlating the difficulty of removing the plug and perhaps explaining most of the difficulties with rf conditioning. A microscope photograph of a portion of the damage area is shown in Figs. 11.

On the surface of the GaAs crystal for Sample 1 could be seen three barely visible specks. Fig. 12 shows electron-microscope photographs of one of these specks.

Finally, the QE was remeasured in the DC gun. The results are shown in Table 6.

Table 6. QE in DC gun before (see Table 5) and after the high power rf tests. The field is 6 MV/m for the “after” measurements.

Sample	Cs layer (nm)	QE at 266 nm	
		Before	After
1	0		$3.7 \times 10^{-6}$
2	10	$2.6 \times 10^{-3}$	$5.2 \times 10^{-4}$

For Sample 2, it is readily seen that the QE has not greatly deteriorated despite the relatively low values measured with the rf gun (a maximum of  $6 \times 10^{-5}$  at 58 MV/m).

Why was the performance of Sample 2 with Cs better than Sample 1 without? As was hinted earlier, it is possible that Sample 1 did not seat properly, causing unusual rf conditioning problems. This occasionally happens with the Cs<sub>2</sub>Te cathodes as well. Further evidence for this scenario is that in the DC gun the dark current for Sample 1 was nearly zero, whereas for Sample 2 with 10-nm cesium it was significantly higher. See Section 4.3. It is also possible that Sample 2 simply had a smoother surface finish, as mentioned in Section 4.1 above.

## 5. Future work

### 5.1. *Mounting the GaAs crystal on an rf plug*

Eventually one should be able to find a way to mount the GaAs crystal in a manner compatible with an rf gun and simultaneously compatible with a proper cleaning and activation method.[43]

Two new mounting methods have been suggested. The first method is to machine a small tab on the metal plug around the edge of the seat for the crystal. After installing the crystal (no *glue*), the tab would be folded over. The top of the plug at the tabs would then be machined to be flush with the surface of the plug. The resulting void behind the crystal could be pumped from the rear through a hollow plug.

The second method is to cover the majority of the active area of the crystal with a mask and then deposit an appropriate material, such as Au, in the crack between the crystal and the plug. Final machining and vacuum pumping would be necessary as for the first method.

The disadvantages of the first method are that the plug material would be restricted to those compatible with a flexible tab, and also that in folding over the tab, one may bury a large amount of contaminants, thus creating a serious virtual leak right at the edge of the GaAs crystal. The second method avoids these problems, but clearly there would have to be some R&D to ensure the cracks are properly filled and that the filling material stays off the crystal and insulating surfaces.

### 5.2. *Cleaning the crystal at low temperatures*

It may be desirable or even necessary to clean the GaAs crystal at low temperature ( $\ll 600^\circ\text{C}$ ). There are several low temperature methods that could be tried.

Ion-bombardment sputtering is a well developed technique.[44] A similar method called ionized controlled etching (ICE) has been developed in the Photoemission Lab at CERN.[30]

At SLAC, cleaning the crystal with atomic hydrogen ( $\text{H}^*$ ) is being investigated.[45] To be most effective, this technique apparently requires the crystal to be held at  $300\text{-}400^\circ\text{C}$ .

### 5.3. *Compatibility of high electric fields with low work function cathodes*

For a polarized electron source, the QE of the GaAs crystal must be high. Since the energy of the exciting photons must be at the band gap, a high QE implies a low work function. Indeed, an NEA surface is desirable. A measurement of the field emission from an NEA surface in the presence of very high rf fields needs to be made. For this test, it is essential that the GaAs crystal be mounted on the plug in a manner that allows a proper surface cleaning and activation.

The maximum field on the SLAC GaAs crystal is about  $1.7\text{ MV/m}$ . It is a DC field. For the CTF rf gun, the maximum field on the cathode will be nearly 60 times greater. It is known that the HV breakdown limit increases when the duty factor of the HV is decreased. For example, for the same environment, the breakdown limit for pulsed HV is higher than DC. For rf fields, the breakdown limit also increases with frequency,[46] although the exact scaling of the breakdown limit with frequency is not well established.[47]

The  $50\text{ nA}$  upper limit for average dark current for long lifetime operation of the GaAs photocathodes in the SLAC polarized electron source may be due entirely to the  $7\text{ MV/m}$  field seen by the stainless steel cathode electrode, not to the NEA surface of the crystal. This is somewhat confirmed by the SLAC experience that installing a new cathode (using a load-lock system) does not change the dark current nor require additional HV conditioning. The maximum field on the cathode of the rf gun is only 15 times higher than the field on the SLAC stainless steel electrode.

Although the vacuum level for an NEA semiconductor surface is by definition below the level of the conduction band minimum in the bulk, the work function itself remains positive at the surface and in value  $\sim 1\text{ eV}$ . In addition, there may be an interfacial barrier between the GaAs and the Cs-oxide overlayer on the order of  $1.2$

eV.[48] The basic Fowler-Nordheim (F-N) relation predicts the field emission should scale as  $\exp\left(-\frac{j^{3/2}}{E_e}\right)$ ,

where  $\phi$  is the work function of the emitting surface, and  $E_e$  is the effective field at the emitting surface, usually expressed as an enhancement of the applied field  $E$ , i.e.,  $E_e = \beta E$ . If one assumes for the test reported here that with cesiated GaAs the effective work function was  $2\text{ eV}$  (as it is for  $\text{Cs}_2\text{O}$ ), then the increase in the field emission for a work function of  $1\text{ eV}$  is only a factor of 7 for the same applied field  $E$ . But in fact, the metallic microprotrusion (MM) model, by which the F-N relation is often interpreted, may not be the best explanation of the field emission process. The metal-insulator-vacuum (MIV) and metal-insulator-metal (MIM) models developed by Latham and co-workers[49] have been very successful in explaining field emission from sites as

empirically found. The expression for field emission derived from these models does not contain the work function of the metallic surface at all. Instead, the work function of micro-particles (0.1-1  $\mu\text{m}$  in size) of polycrystalline and amorphous insulating materials naturally occurring on the surface is contained as a linear term in the exponent of the current-voltage relation. The Cs-oxide layer used to create an NEA surface may perform the role of the insulating material in the MIV and MIM models. It remains to be seen experimentally if the highly-doped GaAs crystals perform the role of the metal substrate or if they act as very large “insulating” crystal with properties for field emission quite different than the naturally occurring micro-particles.

Some indication of the dark current to be expected from a low work function surface in a high field is indicated by the characteristics of an S-20 photodiode. The typical sensitivity of such a photodiode is  $\sim 2$  mA/W at 800 nm, corresponding to a QE of 0.3%. The dark current for an 18-mm cathode is quoted as  $10^{-7}$  A for a field of  $\sim 6$  MV/m (3 kV over a cathode-anode gap of  $\sim 0.5$  mm),[50] which is almost identical to the dark current shown in Fig. 4 for Sample 2 with 10-cm Cs and a similar DC field intensity.

#### 5.4. *High charge measurements at band gap*

Ultimately one must test the properties of an NEA GaAs cathode in the rf gun when excited by a high-power, short-pulse laser that is tuned to the band gap edge. The properties to be tested include the QE, the lifetime, the pulse lengthening, and the cathode charge limit. The relevance of these properties was discussed in Section 2.

The principal problem for conducting these tests at CERN--assuming that it has been found that the QE of an NEA GaAs cathode is not entirely destroyed by the dark current in the environment of an operating rf gun--is the need for a high-power, short-pulse, tunable laser.

The present CTF laser system is a high-power, short-pulse, Nd:YLF laser system. It should be possible to drive a single-pass traveling-wave parametric generator with the CTF laser system to produce the desired pulse structure for testing GaAs. Such an amplifier could presumably be built in the period of about 1 year at a cost in materials of  $< 50000$  CHF. The principal problem for CERN, in addition to the cost, is the lack of manpower for this project. Suitable collaborators might be found to solve this problem.

#### 5.5. *Schedule*

At the end of the 1996 experimental period for Gun 4 and CTF-2, it is tentatively planned to install an activated (NEA surface) GaAs cathode in the gun and measure the resulting dark current. SLAC will participate in providing an activated cathode, perhaps by using a portable carrier that would be mate to the CTF cathode transporter. CERN will investigate cleaning GaAs crystals by the ICE method. The present laser as described in this report is expected to be the only laser available.

The success of the testing in 1996 would provide a strong motivation to develop a high-intensity, short-pulse tunable laser for additional testing of GaAs.

#### 5.6. *International collaboration for an rf gun for polarized electrons*

Responding to the call for international and interlaboratory collaborations in the 1995 report of the Technical Review Committee,[51] and recognizing that there is not now nor likely to be in the near future a single laboratory that will devote the resources necessary to fully investigate the prospects for an rf gun for future colliders that can provide highly polarized electrons, scientists at three laboratories (initially), consisting of CERN, KEK/Nagoya, and SLAC, have agreed to form a collaboration for this purpose. It is expected that future work on polarized rf guns at CERN and SLAC will be carried out as part of this collaboration.

## 5.7. Conclusions

The first test of GaAs in an rf gun has been successfully completed. The GaAs crystals were chemically cleaned before placing them in the vacuum system, but no attempt was made to produce an atomically clean surface preparatory to activation. Both uncesiated and cesiated crystals were tested in the S-band gun at the CLIC Test Facility, the measurements with the former being somewhat suspect because of poor rf contact. RF fields at the surface of the cesiated crystal of  $>50$  MV/m were achieved with minimal rf conditioning. The associated dark current was encouragingly small. Using blue light, some photoemission was observed. There was no detuning of the rf cavity, and despite an extensive amount of rf conditioning with the uncesiated crystal, no deterioration of the rf gun for normal high-power operation with a Cs<sub>2</sub>Te cathode was observed. Future tests, expected to be conducted as part of a larger international collaboration, will include a measurement of the dark current at high field in an rf gun having a GaAs cathode with an NEA surface.

## 6. Acknowledgments

Useful discussions with R. Miller (SLAC) are gratefully acknowledged. We also thank S. Tantawi (SLAC) for pointing out the work of A.M. Vaucher.

## 7. References

- 
- [1] R. Alley et al., "The Stanford linear accelerator polarized electron source," Nucl. Instrum. and Meth. A 365 (1995) 1.
  - [2] J.S. Fraser et al., Proc. 1987 IEEE Particle Accelerator Conference, Washington, DC, p. 1705.
  - [3] GaAs cathodes have so far been rejected for the CTF rf gun for much the same reasons as given in ref. [2].
  - [4] J. Clendenin.
  - [5] J. Clendenin et al., "Prospects for generating polarized electron beams for a linear collider using an rf gun," Nucl. Instrum. and Meth., A340 (1994) 133.
  - [6] A.V. Novokhatski et al., "A laser-driven gun for electron-positron factories," Nucl. Instrum. and Meth., A340 (1994) 237.
  - [7] For example, see G. Wendt, in *Electric Fields and Waves*, v. XVI of S. Flügge, ed., Encyclopedia of Physics (Berlin: Springer, 1958), p. 17.
  - [8] For example, see D.P. Russell III, "High-Brightness Electron-Beam Production at the Brookhaven Accelerator Test Facility," Ph.D. dissertation, Princeton Univ., DOE/ER/3072-67 (January 1992).
  - [9] To properly focus the beam using the CTF gun, the charge is extracted 30° from the zero-crossing of the rf. Thus the accelerating field is approximately half the peak rf field.
  - [10] A "short pulse" as used here is defined as one in which the pulse duration is much less than the cathode-anode transit time.
  - [11] The term "cathode charge limit" derives from the early observations of the phenomenon at SLAC when it was thought that the total charge that could be extracted was subject to a limitation. See M. Woods et al., J. Appl. Phys. 73 (1993) 8531. Here we freely use "cathode current limit" to refer to the current limitations due to the same phenomenon.
  - [12] H. Tang et al., *Fourth European Part. Acc. Conf.*, London, 27 June - 1 July, 1994, eds. V. Sulter and Ch. Petit-Jean-Genaz, p. 46.
  - [13] A model for the cathode charge limit that is consistent with the SLAC measurements is found in A. Herrera-Gómez and W.E. Spicer, Proc. SPIE 2022 (1993) 51.
  - [14] F. Meier and H. Siegmann, "Production and Detection of Spin Polarized Electrons," in M. Chatwell et al., eds., Proc. of the *Workshop on Photocathodes for Polarized Electron Sources for Accelerators*, Stanford, CA, Sept. 8-10, 1993, SLAC-432 Rev. (1994), p. 282.

- 
- [15] D.C. Schultz et al., Proc. *10th Int. Symp. on High Energy Spin Physics*, Nagoya, Japan (Universal Academy Press, Tokyo, 1993), p. 833.
- [16] R.V. Latham and N.S. Xu, *Vacuum* 42 (1991) 1173.
- [17] High-pressure, high-purity water rinsing is a technique developed at CERN to improve the high field performance of superconducting rf cavities. See ref. [18]. The technique has been shown to be equally effective for normal conducting rf cavities. See ref. [19].
- [18] Ph. Bernard et al., "Superconducting Niobium Sputter-Coated Copper Cavities at 1500 MHz," Proc. of the *5th Workshop on RF Superconductivity*, DESY, Hamburg (1991).
- [19] M. Yoshioka et al., Proc. of the *1994 Int. Linac Conf.*, Tsukuba (1994) 302.
- [20] A.V. Aleksandrov et al., *Phys. Rev. E* 51 (1995) 1449.
- [21] Presently, the only proven practical way to activate the MOCVD-grown strained-lattice GaAs crystals is to heat the crystal to 600° C for ~1 hour. This would un-"glue" a crystal from an rf plug.
- [22] S.M. Sze, *Physics of Semiconductor Physics*, 2nd ed., (New York, John Wiley, 1981), Appendix H.
- [23] O. Madelung, ed., *Semiconductors, Group IV Elements and III-V Compounds* (New York: Springer, 1991), p. 101 ff.
- [24] See the discussion in Section 1.8.5 of G.W. Kaye and T.H. Laby, "Tables of Physical and Chemical Constants" (London: Longman, 1986), p. 128.
- [25] J.D. Jackson, *Classical Electrodynamics*, 2nd ed. (New York: John Wiley, 1975), p. 284 ff.
- [26] *CRC Handbook of Chemistry and Physics*, 73rd Ed., 1992-1993, p. 12-108.
- [27] D.A. Fraser, *The Physics of Semiconductor Devices*, 4th ed. (Oxford: Clarendon Press, 1986).
- [28] B.O. Seraphin and H.E. Bennett, "Optical Constants," in R.K. Willardson and A.C. Beer, eds., *Semiconductors and Semimetals*, v. 3: *Optical Properties of III-V Compounds* (New York: Academic Press, 1967), p. 499.
- [29] A. M. Vaucher et al., *IEEE Trans. Microwave Theory Tech.* MTT-31 (1983) 209.
- [30] E. Chevallay et al., *Nucl. Instrum. and Meth. A* 340 (1994) 146.
- [31] A very thin layer of Te ( a few nanometers) is deposited directly on the Cu plug and then a few nanometers of Cs added on top. See G. Suberlucq, "Choix d'une photocathode pour le CLIC Test Facility du CERN," Proc. Journées d'Etude sur la photoémission a Fort Courant, 5 et 6 Avril 1993, Observatoire de Paris, FR, p. 133.
- [32] E.L. Ginzton, *Microwave Measurements* (New York: McGraw-Hill, 1957), p. 439.
- [33] R. Bossart et al., CERN PS 92-19 (LP) and CLIC Note No. 161 (1992).
- [34] Note that if we assume  $\epsilon_{r1}=13$  (the value for intrinsically doped GaAs),  $\Delta f \sim 50$  kHz.
- [35] A "bad" Cs<sub>2</sub>Te cathode was chosen for comparison since no field emission can be observed in the DC gun for "good" Cs<sub>2</sub>Te or bare Cu cathodes.
- [36] H.C. Miller, *Values of Fowler-Nordheim Field Emission Function  $n(y)$ ,  $t(y)$ , and  $s(y)$* , General Electric Technical Information Series No. 66.C-148 (1966).
- [37] A.H. Lumpkin, Conference Record of the *1991 IEEE Particle Accelerator Conf.*, San Francisco, p. 1967.
- [38] At full voltage, the optimum phase for the gun half-cell is 30°. Consequently the field at the cathode during photoémission is approximately one-half the maximum value.
- [39] The streak camera was manufactured by ARP, Strasburg, FR. Its measured resolution was ~4 ps.
- [40] S. Battisti et al., "Magnetic Beam Position Monitors for LEP Pre-Injector," CERN/PS 87-37 (BR), presented at the 1987 Part. Acc. Conf., Washington, D.C., March 16-19, 1987.
- [41] F. Chautard (CERN), private communication.
- [42] The high pressure, ultra-pure water cleaning technique, along with other innovative techniques, was applied to an S-band rf cavity operated at room temperature. If the results are scaled with field, it appears a dark current of ~5 pC/( $\mu$ s of rf) was achieved for 100 MV/m, and essentially zero dark current for 50 MV/m. See ref. [19]. Note that the absolute value

---

of the dark current in ref. [19] is subject to a large uncertainty (H. Matsumoto, private communication, CERN, February 1996).

[43] It may also be possible to grow a GaAs crystal on a metal substrate. This may be no more difficult than the already highly successful use of glass as the substrate (used for night-vision devices).

[44] J.S. Escher, "NEA Semiconductor Photoemitters," in *Semiconductors and Semimetals*, v. 15, eds. R.K. Willardson and A.C. Beer (Academic Press, New York, 1981), p. 216.

[45] "On the Use of Atomic Hydrogen in MBE," EPI Application Note (EPI, 1290 Hammond Rd., St. Paul, MN 55110, August/September 1994)

[46] R.V. Latham, in R.V. Latham, ed., *High Voltage Vacuum Insulation* (London, Academic Press, 1995), p. 54.

[47] No sign of rf breakdown or need to condition rf components was observed at CTF-1 for 20 ns, 30-GHz rf pulses up to peak powers of 60 MW, corresponding to peak surface fields of 250 MV/m. I. Wilson, CERN (1996) private communication.

[48] J.J. Uebbing and L.W. James, *J. Appl. Phys.* 41 (1970) 4505.

[49] N.S. Nu, in R.V. Latham, ed., *High Voltage Vacuum Insulation* (London, Academic Press, 1995), p. 115.

[50] For example, see specifications for PD-18, Photek Limited, 26 Castleham Rd., St. Leonards-on-Sea, East Sussex TN38 9NS, UK.

[51] "Present and Future Areas of Collaboration," ch. 5 of *International Linear Collider Technical Review Committee Report 1995*, Prepared for the Interlaboratory Collaboration for R&D Towards TeV-scale Electron-Positron Linear Colliders, SLAC-R-95-471.